www.ijecs.in
International Journal Of Engineering And Computer Science ISSN:2319-7242
Volume 2 Issue 8 August, 2013 Page No. 2397-2402

Analysis Of Full Bridge Boost Converter For Wide Input Voltage Range

Ch. Abhilash[1], R. Shirisha[2], Khaja Rafi[3]

[1]Dept. of Electrical and electronic engineering, CMRCET, Hyderabad.
abhilash.chandolu@gmail.com

[2]Assistant Professor, Dept. of Electrical and electronic engineering, CMRCET, Hyderabad.
shirireddy42@gmail.com

[3]Assistant Professor, Dept. of Electrical And Electronic Engineering, CMRCET, Hyderabad.
khaja.rafi@gmail.com

Abstract: A family of isolated dc/dc converters for wide input-voltage range is proposed in this paper, and the full-bridge(FB) boost converter, being one of the typical topologies, is analyzed. Due to the existence of the resonant inductor (including the leakage inductor), the FB-boost converter can only adopt the two-edge-modulation (TEM) scheme with the FB cell being leading-edge modulated and the boost cell being trailing-edge modulated to minimize the inductor current ripple over the input-voltage range, and a phase-shift-control-scheme-based TEM is proposed which realizes phase-shifted control for the FB cell to achieve zero-voltage switching. In order to improve the reliability and efficiency of the FB-boost converter, a three-mode dual-frequency control scheme is proposed, in which the FB-boost converter operates in boost, FB-boost and FB modes in low, medium and high input voltage regions, respectively, and for which the expression of the inductor current ripple is derived in this paper. A 250–500 V input, 360 V output, and 6 kW rated power prototype is fabricated to verify the effectiveness of the design and control method.

Keywords**:** Isolated buck–boost converter, full bridge boost converter, leakage reactance, two-edge modulation(TEM).

I. INTRODUCTION

The use of renewable energy has recently received worldwide attention in view of the continuous growth in energy consumption and the pressing need for reducing carbon emission to the atmosphere. Photovoltaic (PV) power has been a promising renewable energy source due to its zero pollution (both air and noise), ability to operate with much less restriction on location, and ease of maintenance. Nowadays, the grid-connected PV system has become an important means of PV power utilization.

The grid-connected inverter, being an essential part of the grid-connected PV system, has profound impact on the overall efficiency and cost of the system. Currently, the most popular configuration of the two-stage grid-connected inverter is a cascade configuration consisting of a front-end dc/dc converter and a downstream inverter. The front-end dc/dc converter performs two major tasks: 1) to produce voltage at appropriate level to the downstream inverter; 2) to extract maximum power from the PV arrays. The downstream inverter then converts the dc output voltage of the front-end dc/dc converter into the ac grid connected voltage. An isolated dc/dc converter with HF transformer can be used as the front-end dc/dc converter.

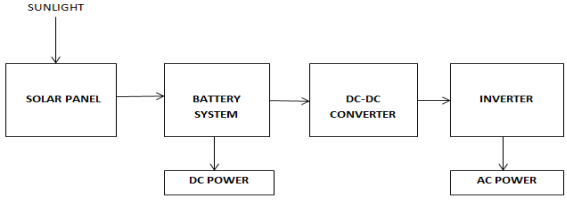

Figure 1: Block diagram of PVEC System.

It is well known that the output voltage of PV arrays fluctuates with the output current and climate conditions such as solar radiation and ambient temperature. In other words, the output voltage of PV arrays has a wide variation range. It is thus imperative for the front-end dc/dc converter to achieve a high efficiency over the entire input-voltage range. It is known that the buck converter has the ability of voltage step down, and the efficiency decreases with increasing input voltage, whereas the boost converter has the ability of voltage step up, and the efficiency increases with increasing input voltage and a two state buck–boost(TSBB) converter have the ability of voltage step up and down.

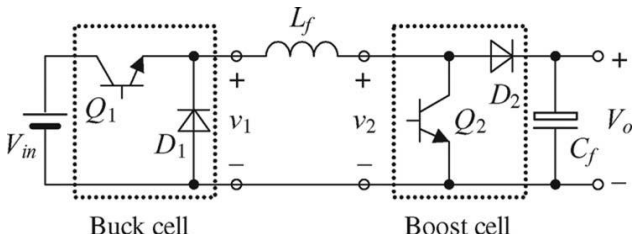

Figure 2: TSBB converter

II. Derivation Of Isolated Dc/Dc Converter

In the TSBB converter shown in Fig. 2, Q_1 and D_1 form the buck cell, and Q_2 and D_2 form the boost cell. Galvanic isolation can be realized by inserting an HF transformer into the TSBB converter, either in the buck cell or the boost cell, leading to the buck-derived isolated cell or the boost-derived isolated cell, respectively. Fig. 3 shows the isolated dc/dc converter, which is obtained by replacing the buck cell with the FB cell. This converter is called *FB-boost converter*.

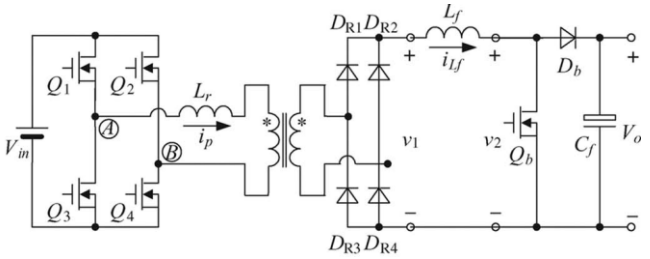

Figure 3: FB-boost converter

In Fig. 3, the body diodes and junction capacitors of power switches $Q1$ to $Q4$ are omitted for brevity, and Lr is the resonant inductor which includes the leakage inductor of the transformer to achieve zero voltage switching (ZVS) for the power switches in the FB cell.

It should be noted that if the resonant inductor is removed and the leakage inductor of the transformer is zero, the control strategy for the TSBB converter is effective for the FB boost converter. However, the leakage of the transformer is inevitable in the practical circuits, and for the FB converter, an external resonant inductor is added in series with the primary of the transformer to achieve ZVS for the power switches generally.

III. Comparison Of Voltage Conversion In Buck-Boost And FB-Boost Converters

1) Two State Buck-Boost Converter

If the active switches Q_1 and Q_2 of the TSBB converter are switched ON and OFF simultaneously, the operating principle is the same as the inverting buck–boost converter. In fact,Q_1 and Q_2 can be controlled independently. As seen in Fig. 2, by neglecting the ripple of the inductor current i_{Lf}, the average inductor current I_{Lf} equals to $I_o/(1-d_2)$, where I_o is the output current, and d_2 is duty cycle of Q_2.

Therefore, reducing d_2 will reduce I_{Lf}, as a result, the conduction losses in the inductor and power switches are reduced. Thus, d_2 should be as small as possible. The voltage conversion of the TSBB converter is $V_o/V_{in} = d_1/(1-d_2)$, where d_1 is duty cycle of Q_1.

2) FB-Boost Converter

Due to the presence of the resonant inductor Lr in the FB cell, the actual duty cycle of $v1$ is smaller than the duty cycle of v_{AB}. This is the phenomenon of *duty-cycle loss*, which can be expressed as

$$D_{\text{loss}} = 4kL_r I_{Lf\_av} f_s / V_{\text{in}} \quad \text{---------- (1)}$$

Where $I_{Lf\text{-av}}$ is the average current of inductor Lf ,k is the turns ratio of the secondary to primary windings of the transformer, and fs is the switching frequency of the FB cell.

As shown in Fig. 3, the inductor current, iLf, flows into the load through diode Db only when Qb is switched off. Thus, the average inductor current is

$$I_{Lf\_av} = \frac{I_o}{1-d_2} \quad \text{---------- (2)}$$

Where Io is the output current, and $d2$ is the duty cycle of Qb. Substitution of (2) into (1) gives

$$D_{\text{loss}} = \frac{4kL_r I_o f_s}{V_{\text{in}}(1-d_2)} \quad \text{---------- (3)}$$

Also, the average voltages at the two terminals of the inductor Lf are

$$\bar{v}_1 = (d_1 - D_{\text{loss}})kV_{\text{in}} = d_{1\_\text{eff}} kV_{\text{in}} \quad \text{---------- (4)}$$

$$\bar{v}_2 = (1-d_2)V_o \quad \text{---------- (5)}$$

Where $d1$ is the duty cycle of the FB cell, i.e., the duty cycle of vAB, $d1_{\text{eff}} = d1 - D_{\text{loss}}$ is the effective duty cycle of the FB cell, i.e., the duty cycle of $v1$.

The pulsating frequency of the voltage $v1$ is $2fs$, and the pulsating frequency of $v2$ is the switching frequency of Qb, which is denoted as $fs\ b$. Setting $fs\ b = 2fs$ would optimize the design of Lf . In the following discussion, it is assumed that $fs\ b = 2fs$. At steady state, the volt–second product of Lf is zero in every switching period of Qb, implying that the average voltage at the two terminals of Lf are equal, i.e.,

$$\bar{v}_1 = \bar{v}_2. \quad \text{---------- (6)}$$

By substituting (3), (4), and (5) into (6), the expression of the output voltage is derived as

$$V_o = \frac{d_{1\_\text{eff}}}{1-d_2} kV_{\text{in}} = \frac{d_1}{1-d_2} kV_{\text{in}} - \frac{4k^2 L_r I_o f_s}{(1-d_2)^2}. \quad \text{----------(7)}$$

It can be seen from (7) that the output voltage of the FB-boost converter is not only related to the duty cycles of the FB cell and boost cell, but also related to the output current, the resonant inductor and the switching frequency.

Thus, in the TSBB converter, the boundary input voltage of the buck mode and boost mode is a point but for the FB-boost converter, due to the existence of the resonant inductor, the boundary input voltage of the FB mode and boost mode is not a point any longer, and it is more efficient than TSBB converter.

IV. Phase-Shift Tem To Minimize The Inductor Current Ripple

The FB-boost converter can adopt the TEM scheme with the FB cell being leading-edge modulated and the boost cell being trailing-edge modulated. Fig. 4 illustrates the TEM scheme where the FB cell is leading-edge modulated and the boost cell is trailing-edge modulated.

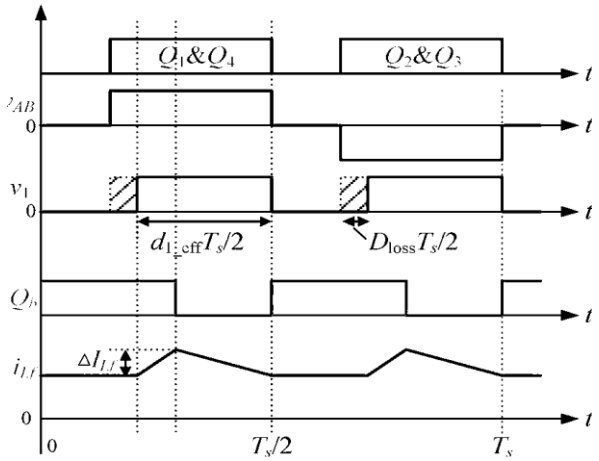

Figure 4: FB cell being leading-edge modulated and boost cell being trailing-edge modulated.

As the trailing edge of *v*1 is fixed, the overlapping conduction time of the diagonal switches of the FB cell and *Qb* is kept unchanged even when D_{loss} is nonzero. Thus, the inductor current ripple does not change with D_{loss}, and is only determined by $d1_{\ eff}$.

It can be seen from (2) that in order to reduce the average inductor current, *d*2 should be as small as possible. According to (7), larger $d1_{\ eff}$ means smaller *d*2. When $kVin \le Vo$,$d1_{\ eff} + d2 \ge 1$. Due to the nonzero D_{loss}, the maximum value of $d1_{\ eff}$ is $1-D_{loss}$.

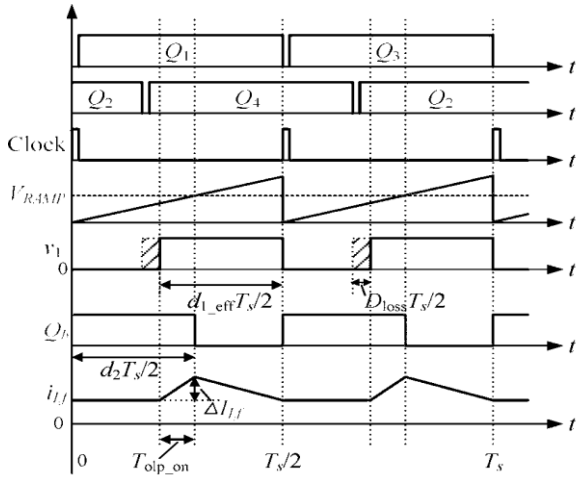

Figure 5(a): $kVin \le Vo$

Thus, the FB cell is set to work at full duty cycle, i.e., *d*1 = 1, and the duty cycle of the boost cell, *d*2, is controlled to regulate the output voltage, and the FB-boost converter acts as a boost converter. This operation mode is defined as the *boost mode*. Substituting *d*1 = 1 or $d1_{\ eff} = 1-D_{loss}$ into (7) yields

$$V_o = \frac{1-D_{loss}}{(1-d_2)}kV_{in} = \frac{kV_{in}}{(1-d_2)} - \frac{4k^2L_rI_of_s}{(1-d_2)^2} \quad \text{--------(8)}$$

When $kV_{in} > Vo$, $d1_{\ eff} + d2 < 1$, i.e., $d2 < 1 - d1_{\ eff}$. Two cases can be identified for this condition. In the first case, *d*2 is greater than 0 even when *d*1 reaches 1 in order to obtain the required output voltage. In the second case, *d*2 can be zero and *d*1 is controlled to regulate the output voltage.

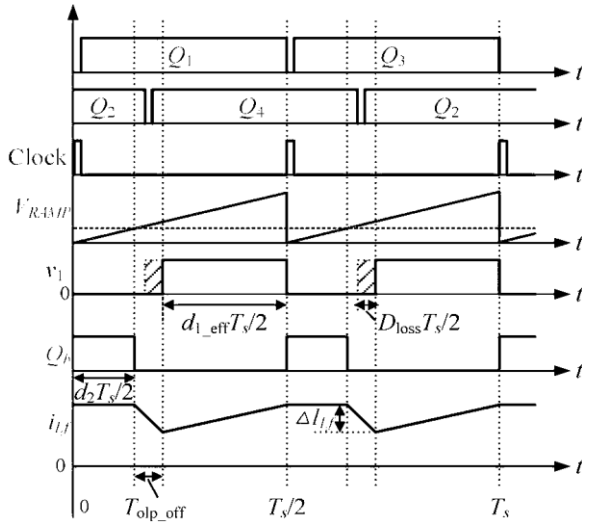

Figure 5(b): $kVin > Vo$

For the first case, the expression of the output voltage is the same as that shown in (8). Substituting *d*2 = 0 into (8), the boundary input voltage for the two cases is

$$kV_{in\_b} = \frac{V_o}{1-D_{loss}} = V_o + 4k^2L_rI_of_s \quad \text{----------(9)}$$

When $Vo < kV_{in} < Vo + 4k^2Lr\ Io\ fs$, *d*2 is greater than 0 with *d*1 being 1, the FB-boost converter operates in the boost mode, as discussed above. Thus, the input-voltage range for the boost mode is expanded from $kVin < Vo$ to $kVin < Vo+4k^2LrIo\ fs$.

When $kVin \ge Vo+4k^2Lr\ Io\ fs$,*d*2 can be as small as 0. In this case, *Qb* of the boost cell is off, and *d*1 is controlled to regulate the output voltage, and the FB-boost converter thus acts as an FB converter. This operating mode is defined as the *FB mode.* Substituting *d*2 = 0 into (7), we get

$$V_o = d_{1\_eff}\ kV_{in} = d_1kV_{in} - 4k^2L_rI_of_s \quad \text{-------(10)}$$

Since there are two operating modes over the input-voltage range, this control scheme is called two-mode PS-TEM. Combining (11) and (13), the voltage conversion for the FB-boost converter with two-mode PS-TEM is

$$V_o = \begin{cases} \dfrac{kV_{in}}{(1-d_2)} - \dfrac{4k^2L_rI_of_s}{(1-d_2)^2}, & kV_{in} \le V_o + 4k^2L_rI_of_s \\ d_1kV_{in} - \ 4k^2L_rI_of_s, & kV_{in} > V_o + 4k^2L_rI_of_s \end{cases} \quad \text{-----(11)}$$

V. THREE-MODE DUAL-FREQUENCY PS-TEM CONTROL SCHEME

In order to solve the problems of two-mode PS-TEM control, a third region of [Vin_b_{min}, $Vin\ b_{max}$] is introduced. In this region, the FB cell works at a fixed maximum duty cycle $d1_{\ max}$, so that the duty cycle of the boost cell, *d*2 , is set as small as possible in order to reduce the average inductor current, and at the same time *d*2 is controlled to regulate the output voltage. This operating mode is defined as the FB-boost mode. Therefore, the input-voltage range is divided into three regions, i.e., $Vin \le Vi_{n\ bmin}$ for the boost mode, $V_{in\ bmin} < Vin \le V_{inbmax}$ for the FB-boost mode, and $Vin > V_{in\ bmax}$ for the FB mode.

In order to verify the operating principle of the FB-boost converter and the effectiveness of the control scheme, a

250−500 V input, 360 V output, and 6 kW rated power prototype is fabricated. As mentioned above, in the FB-boost mode, *d*1 should be made as large as possible to reduce *d*2. We set the minimum value of *d*2 as 0.05 in this paper. Substituting V_{inbmax} = 376V, *Io* = 0.10 ×16.7 = 1.67 A, and *d*2 = 0.05 into (8) yields *d*1 = 0.92, substituting *k* = 1 and *d*1 max= 0.92, the voltage conversion of the FB-boost converter under three-mode PS-TEM control is

$$V_o = \begin{cases} \dfrac{V_{in}}{1-d_2} - \dfrac{4L_rI_of_s}{(1-d_2)^2} & V_{in} \le 362V \\ \dfrac{0.92V_{in}}{1-d_2} - \dfrac{4L_rI_of_s}{(1-d_2)^2} & 362V < V_{in} \le 376V \\ d_1V_{in} - 4L_rI_of_s & \ge 376V \end{cases} \quad -(12)$$

VI. CIRCUIT DIAGRAM AND EXPERIMENTAL RESULTS

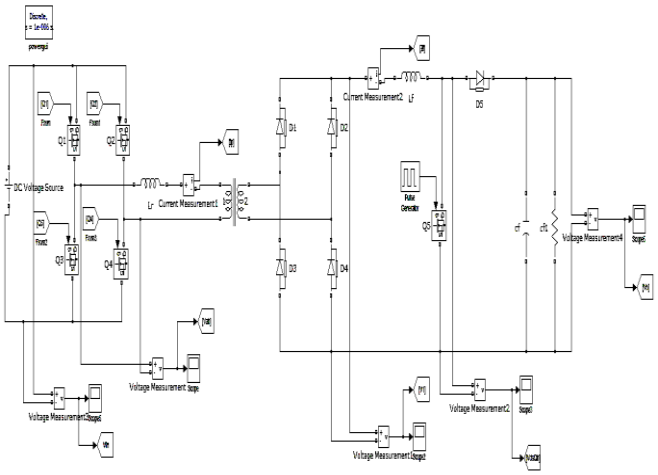

Figure 6(a): Simulink model of FB-Boost

Fig 6(a) shows the simulation circuit of FB-Boost circuit. The values of the components are shown in the appendices of the thesis. The circuit has a full bridge of four switches which converts DC to AC and the output is sent through the transformer then a diode bridge is present to convert it again to DC and then the boost cell is present.

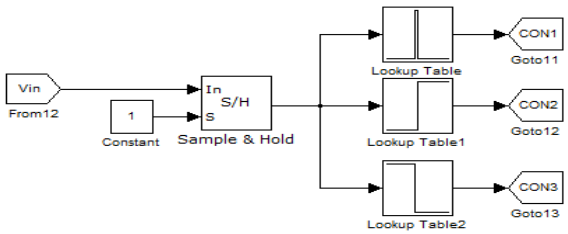

Figure 6(b): Selection of mode

The fig 6(b) gives the selection of mode or operation of the circuit based on the input voltage the selection of mode is shown in the tabular column below

Table 1: Mode Selection

$V_0 < 362$	$362 \le V_0 < 376$	$V_0 > 376$
Con 1 is low	Con 1 is high	Con 1 is low
Con 2 is low	Con 2 is low	Con 2 is high
Con 3 is high	Con 3 is low	Con 3 is low

The input voltage, as obtained by the voltage sampling cell, is sent to the control block, i.e., *Vin* /*H*, where *H* is the sampling coefficient. Also, *Vb* 1 and *Vb* 2 correspond to the minimum and maximum values of the boundary input voltage divided by *H*, respectively, i.e., *Vin* bmin/*H* and *Vin* bmax/*H*. The operating mode of the FB-boost converter can be determined by comparing *Vin* /*H*, given *Vb* 1 and *Vb* 2 . Furthermore, CON1, CON2 and CON3 are the operating mode selection signals corresponding to the FB mode, boost mode, and FB-boost mode, respectively.

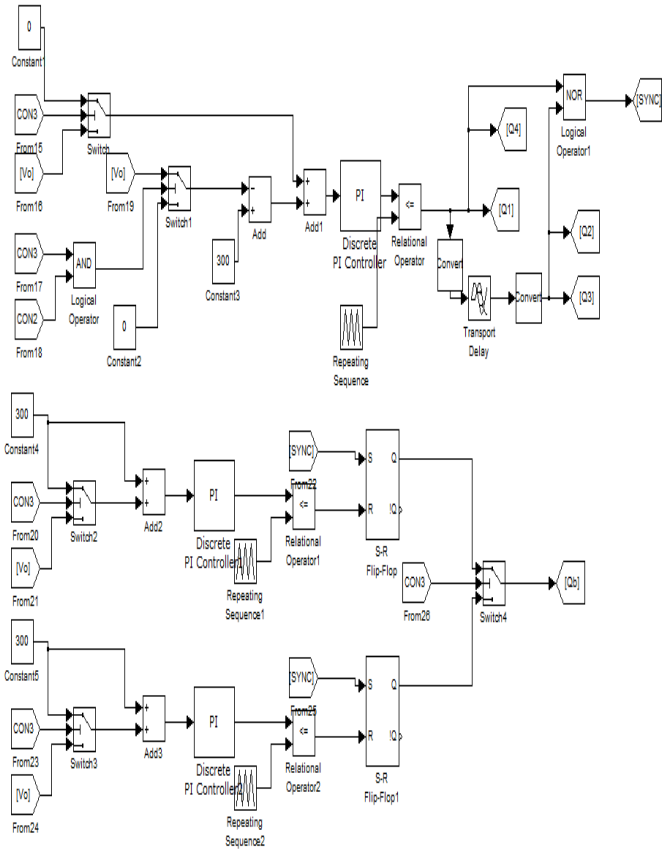

Figure 6(c): Control circuit for FB-cell and boost cell

The above figure 6(c) shows the control circuit for the FB-Boost converter the upper one in the fig is the control circuit for FB cell switches i.e. Q1-Q4 switches. The below circuit is the control circuit for boost cell. Both the circuits are useful to produce signals for the respective switches the time period is varied according to the values derived theoretically in the before chapters. The signals for the switches are produced by PWM technique.

*Q*1 and *Q*3 are the drive signals for the leading switches of the FB cell, and *Q*2 and *Q*4 are the drive signals for the lagging switches of the FB cell. The drive signals *Q*1 and *Q*3 are sent to the NOR gate, giving a pulse signal with the pulse width equal to the dead time of *Q*1 and *Q*3 . This pulse signal is then sent to the *SYNC* pin as the synchronization signal for the boost cell, thus achieving TEM for the FB-boost converter. There are two separate output voltage regulating circuits for the

FB cell and the boost cell. In the FB mode, CON1 is at high level, and CON2 and CON3 are at low level. The signal switch *S*3 is turned on, pulling down the voltage of the non inverting terminal of the boost-cell regulator to zero. Thus, the output of the boost-cell regulator is forced to zero, and the duty cycle *d*2 is zero accordingly.

Moreover, the FB-cell regulator determines the duty cycle of the FB cell. In the boost mode, CON2 goes high, and CON1 and CON3 goes low. The signal switch makes the control circuit of the FB-cell regulator to go below *V*ref . Thus, the FB-cell regulator is saturated, and the duty cycle of the FB cell reaches its maximum value of 1. Meanwhile, the boost-cell regulator determines the duty cycle of the boost cell. In the FB-boost mode, CON3 is at high level, and CON1 and CON2 are at low level. Both the control circuits are turned on, and the FB-cell regulator 1 is saturated and its output voltage is clamped letting the FB cell operate at the maximum duty cycle of *d*1 max.

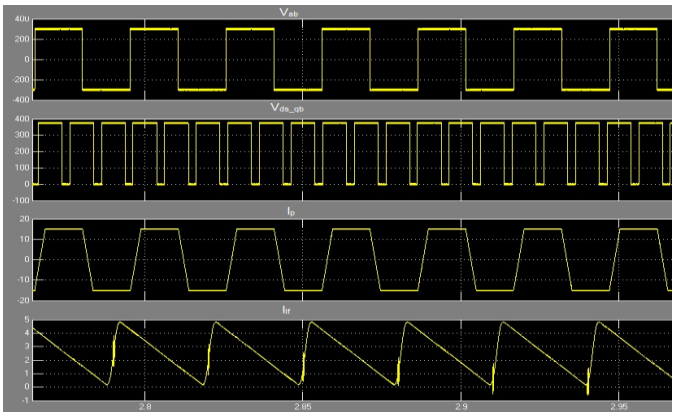

Figure 7(a): Boost mode (V_{ab} in volts; V_{ds_qb} in volts; I_p in amps; I_{lf} in amps).

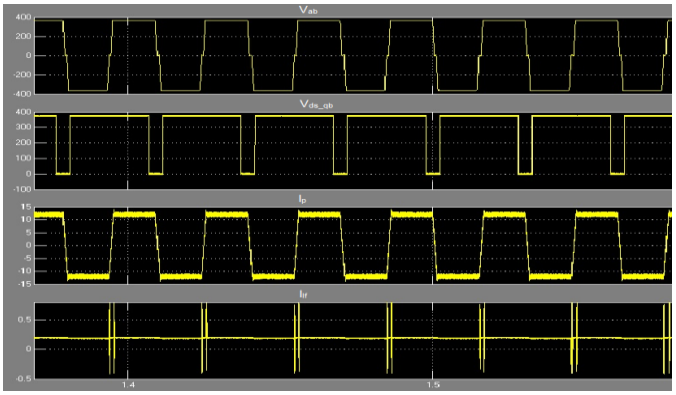

Figure 7(b): Full bridge-boost mode (V_{ab} in volts; V_{ds_qb} in volts; I_p in amps; I_{lf} in amps).

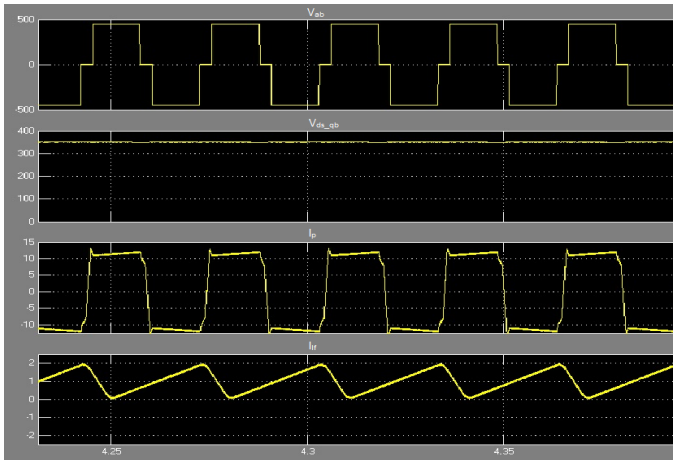

Figure 7(c): Full bridge mode (V_{ab} in volts; V_{ds_qb} in volts; I_p in amps; I_{lf} in amps).

The figures of 7 are the experimental waveforms of FB-Boost converter under three mode dual frequency PS-TEM control which include the primary voltage Vab of the FB cell, drain to source voltage of Qb of the boost cell, Vdsqb, and inductor current Ilf (only ac component) from top to bottom in each figure. Fig. 7(a) shows the waveforms at Vin = 300 V, with the FB-boost converter operating in the boost mode. It can be seen that the duty cycle of the FB cell is 1, and Vo is regulated by controlling the duty cycle of the boost cell. Fig. 7(b) shows the waveforms at Vin = 365 V, with the converter operating in the FB-boost mode. The FB cell operates at a fixed maximum duty cycle of 0.92. Since Vin is close to Vo , the inductor current ripple is nearly zero. Fig. 7(c) shows the waveforms at Vin = 450 V. Here, the converter operates in the FB mode, the boost cell quit working, and Vo is regulated by controlling the duty cycle of the FB cell. It can be seen that the primary current of the transformer is symmetrical in every two switching periods of the boost cell.

VII. CONCLUSION

A family of isolated buck–boost converters is proposed in this project for use in applications where the input-voltage range is wide and galvanic isolation is required. For illustration, a FB boost converter version is analyzed. Since the boundary input voltage of the FB mode and boost mode changes with the output current due to the resonant inductor, a three-mode PS-TEM control scheme is proposed to improve the efficiency and reliability, in which the converter operates in boost, FB-boost, and FB modes in the lower, medium, and higher input voltage regions respectively, and for which the expressions of the voltage conversion are all derived.

VIII. REFERENCES

[1] Chuan Yao, Xinbo Ruan, Senior Member, IEEE, Xuehua Wang, and Chi K. Tse, Fellow, IEEE, "Isolated Buck–Boost DC/DC Converters Suitable for Wide Input-Voltage Range," IEEE Transactions On Power Electronics, vol. 26, no. 9, September 2011.

[2] T. Shimizu, O. Hashimoto, and G. Kimura, "A novel high-performance utility-interactive photovoltaic inverter system," IEEE Trans. Power Electron.,vol. 18, no. 2, pp. 704–711, Mar. 2003.

[3] M. J. V. Vazquez, J. M A. Marquez, and F. S. Manzano, "A methodology for optimizing stand-alone PV-System sizing using parallel-connected dc/dc converter," IEEE Trans. Ind. Electron., vol. 55, no. 7, pp. 2664– 2673, Jul. 2008.
[4] T. Kerekes, R, Teodorescu, M. Liserre, C. Klumpner, and M. Sumner, "Evaluation of three-phase transformer less photovoltaic inverter topologies," IEEE Trans. Power Electron., vol. 24, no. 9, pp. 2202–2211, Sep. 2009.
[5] F. Blaabjerg, Z. Chen, and S. B. Kjaer, "Power electronics as efficient interface in dispersed power generation systems," IEEE Trans. Power Electron., vol. 19, no. 5, pp. 1184–1194, Sep. 2004.
[6] W. Xiao, N. Ozog, and W. G. Dunford, "Topology study of photovoltaic interface for maximum power point tracking," IEEE Trans. Ind. Electron., vol. 54, no. 3, pp. 1696–1704, Jun. 2007.
[7] M. Pipattanasomporn, M. Willingham, and S. Rahman, "Implications of on-site distributed generation for commercial/ industrial facilities," IEEE Trans. Power Syst., vol. 20, no. 1, pp. 206–212, Feb. 2005.
[8] B. Yuan, X. Yang, D. Li, and Z. Wang, "A new architecture for high efficiency maximum power point tracking in grid-connected photovoltaic system," in Proc. CES/IEEE IPEMC, 2009, pp. 2117–2121.